Pion-nucleon charge exchange and scattering at low energies

P. B. Siegel and W. R. Gibbs
Theoretical Division, Los Alamos National Laboratory, Los Alamos, New Mexico 87545
and Physics Department, Arizona State University, Tempe, Arizona 85721
(Received 12 November 1985)

An analysis of low energy pion-nucleon charge exchange and elastic scattering data is presented. A system of coupled channels with nonlocal potentials is used to include the effects of the Coulomb interaction, pion and nucleon mass differences, and the photoabsorption channel. By using recent accurate charge exchange data, redundancies exist, allowing cross checks between data sets. The cross section for $\pi^+ n \to \pi^0 p$ is deduced and a value of $a_1 - a_3 = 0.290 \pm 0.008\ \mu^{-1}$ is extracted.

I. INTRODUCTION

Recent innovations of pion detection systems have enabled high precision measurements of pion cross sections to be performed. In particular the new π^0 spectrometers are able to accurately measure single charge exchange cross sections on the nucleon. A distinct feature of these charge exchange measurements is the sharp minimum of the forward cross section, $\sigma(0)$, observed at $T_\pi \sim 45$ MeV, which arises from the near cancellation of the s- and p-wave amplitudes. This same dramatic feature has also been observed in pion-nucleus charge exchange reactions, with the minimum somewhat shifted in energy and the shape slightly modified. A possible application of this observation is that $\pi^+ N(A,Z) \to \pi^0 N(A,Z+1)$ isobaric analog state (IAS) reactions might be measured with sufficient accuracy in this energy region to utilize the sensitivity of the s-p cancellation for determining nuclear medium effects on the pion-nucleus interaction. Experiments of this type have been done[1] on ^{7}Li, ^{14}C, ^{15}N, ^{39}K, ^{48}Ca, and ^{120}Sn for $30 < T_\pi < 70$ anticipating the enhancement of our understanding of multiple scattering effects, valence neutron densities, and other nuclear effects on the reaction. In order to isolate these medium effects it is essential to have a good representation for single charge exchange from free nucleons. A precise determination of the minimum of the forward excitation function is required for the reaction $\pi^+ n \to \pi^0 p$ for comparison with reactions on nuclear targets. Unfortunately, this cross section is not directly measurable in the laboratory due to the requirement of a neutron target. However, the charge exchange reaction $\pi^- p \to \pi^0 n$ can be measured and the resulting amplitudes related to those needed for computing the scattering that occurs in the nucleus. Due to the extreme cancellation of the amplitudes, isospin breaking effects (such as mass differences and the Coulomb interaction) need to be considered in transforming from the $\pi^- p \to \pi^0 n$ to the $\pi^+ n \to \pi^0 p$ system. In this paper we will examine some of these effects.

In Sec. II, we present some forms for the parametrization of the two channel S matrix, and estimate how isospin breaking effects alter those parameters. We will also include the effects of the γn channel. In Sec. III, π-N potentials, consistent with single charge exchange data, will be used as a basis for examining the existing pion-nucleon data. We find the redundancy introduced when one assumes isospin invariance of the strong interaction very valuable for comparing data sets. Section IV treats the $\pi^- p \to \pi^0 n$ and $\pi^+ n \to \pi^0 p$ excitation functions and amplitudes in the energy region $30 < T_\pi < 70$ MeV. Simple formulae for the charge exchange amplitudes are given at the end of this section.

II. PARAMETRIZATION OF PION-NUCLEON SCATTERING

Parametrizations of the S matrix of the pion-nucleon system have been discussed by many authors.[2-8] A standard approach is to work within the framework of a coupled-channel potential model using an energy-independent square-well potential to represent the pion-nucleon interaction. One advantage of this method is that the Coulomb field and mass differences, which cause a breaking of the isospin symmetry, can be included in a straightforward manner. The modifications of the S-matrix parameters due to these isospin breaking effects can then be calculated in a relatively unambiguous way. In this section we will apply these ideas to a nonlocal potential, and also estimate the effect of the γn channel on the parametrization of the low energy π-N S matrix. This section presents the foundations of the analysis in some detail. Those readers interested only in the results should skip to Sec. III. We begin by reviewing some basic ideas.

If one assumes the conservation of angular momentum and parity, i.e., $[H,J]=[H,P]=0$, then the full S matrix can be broken down into channels of good angular momentum and parity. Under the further assumption of time reversal invariance, $[H,T]=0$, each J^p channel of the S matrix is required to be symmetric. Finally, the mathematical condition that one has included all existing coupled states is that S be unitary. Thus, if there are n coupled channels for a particular J^p value of S, then

$$S^{JP} \in \left\{ \begin{matrix} \text{symmetric unitary} \\ n \times n \text{ matrices} \end{matrix} \right\} .$$

Consider first the two channel $\pi^- p, \pi^0 n$ ($\pi^+ n, \pi^0 p$) sys-

tem. For pion laboratory energies less than 70 MeV, s- and p-wave scattering dominate, and we will confine our coupled channel analysis to these l values. The scattering is then described by three 2×2 matrices corresponding to good J and P (or l), denoted by S^{lj}: $S^{S_{1/2}},S^{P_{1/2}},S^{P_{3/2}}$. Since a general $n\times n$ symmetric matrix can be parametrized by $n(n+1)/2$ real variables, three parameters are necessary for each S^{lj} matrix for the $(\pi^-\mathrm{p},\pi^0\mathrm{n})$ system. Of the many parametric choices, the form of Blatt and Biedenharn[9] (see also Ref. 3) is very convenient. Their representation of the S matrix uses two eigenphases and a mixing angle:

$$S^{lj}=M_2^T(\epsilon)\begin{bmatrix}e^{2i\delta_1} & 0\\ 0 & e^{2i\delta_2}\end{bmatrix}M_2(\epsilon)$$

where $M_2\in\mathrm{O}(2)$,

$$M_2(\epsilon)=\begin{bmatrix}\cos\epsilon & \sin\epsilon\\ -\sin\epsilon & \cos\epsilon\end{bmatrix}.$$

or

$$S=\begin{bmatrix}e^{2i\delta_1}\cos^2\epsilon+e^{2i\delta_2}\sin^2\epsilon & \frac{1}{2}\sin2\epsilon(e^{2i\delta_1}-e^{2i\delta_2})\\ \frac{1}{2}\sin2\epsilon(e^{2i\delta_1}-e^{2i\delta_2}) & e^{2i\delta_1}\sin^2\epsilon+e^{2i\delta_2}\cos^2\epsilon\end{bmatrix}. \tag{1}$$

In this form, the mixing matrix

$$M_2(\epsilon)=\begin{bmatrix}\cos\epsilon & \sin\epsilon\\ -\sin\epsilon & \cos\epsilon\end{bmatrix}$$

connects the charge (or physical) basis to a basis in which the S matrix is diagonal. For the π-N system in the absence of isospin breaking effects, the eigenphases δ_1 and δ_2 correspond to isospin $\frac{3}{2}$ and $\frac{1}{2}$ phases. In this limit, $\epsilon=\epsilon_I\equiv\sin^{-1}(\sqrt{2/3})$ (or $\epsilon_I\sim54.7$ deg) determined from the Clebsch-Gordan coefficients of the underlying SU(2) isospin symmetry for three pion and two nucleon states. Thus, a quantitative measure of isospin breaking can be obtained by using this parametric form. For low energy pion nucleon scattering, nine parameters are necessary to describe the data (at each energy): six eigenphases $(\delta_{1/2},\delta_{3/2},\delta_{33},\delta_{31},\delta_{13},\delta_{11})$ and three mixing angles $(\epsilon_S,\epsilon_{P1/2},\epsilon_{P3/2})$, each of which become exactly ϵ_I if $[H,I]=0$. We will now consider the following questions:

1. How do the mixing angles, ϵ, depend on energy, π-nucleon off-shell range, etc.?

2. How does including nγ production (i.e., a three-channel S matrix) modify the variables of Eq. (1) $[S^{lj}(\delta_1,\delta_2,\epsilon)]$?

The basis for our calculations will be a coupled channel system of equations of the following form:

$$\begin{aligned}&\nabla^2\psi_1+k_1^2\psi_1+2\mu_1V_{11}\psi_1+2\mu_1V_{12}\psi_2+2\mu_1V_{\mathrm{Coul}}\psi_1=0\ ,\\ &\nabla^2\psi_2+k_2^2\psi_2+2\mu_2V_{22}\psi_2+2\mu_2V_{21}\psi_1=0\ ,\end{aligned} \tag{2}$$

where

$$k_i^2=[s-(m_1^i+m_2^i)^2][s-(m_1^i-m_2^i)^2]/4s\ ,$$

$\sqrt{s}$ is the total invariant energy, and

$$\mu_i=\frac{E_1^iE_2^i}{E_1^i+E_2^i}$$

(the reduced energy in the center of mass for channel i), where $E_i=(m_i^2+k_i^2)^{1/2}$, ψ_1 is the π^-p relative wave function, and ψ_2 is the π^0n relative wave function, with the appropriate boundary conditions.

The hadronic potential V is determined from individual isospin potentials mixed under the assumption of isospin invariance:

$$V=\begin{bmatrix}V_{11} & V_{12}\\ V_{21} & V_{22}\end{bmatrix}=M_2^T(\epsilon_I)\begin{bmatrix}U_{3/2} & 0\\ 0 & U_{1/2}\end{bmatrix}M_2(\epsilon_I)\ ,$$
$$V_{ij}=V_{ji}\ .$$

Note that in Eq. (2) if $V_{\mathrm{Coul}}=0$, $\mu_1=\mu_2$, and $k_1=k_2$, then the S matrix parameters become $\delta_1=\delta_{3/2}$, $\delta_2=\delta_{1/2}$, and $\epsilon_s=\epsilon_I$. The inclusion of the Coulomb potential or $k_1\neq k_2$, due to mass differences between the two channels, will result in general in changes of δ_1 from $\delta_{3/2}$, δ_2 from $\delta_{1/2}$, and ϵ from ϵ_I reflecting the degree of isospin breaking due to these two effects. The energy independent isospin potentials are taken to be of the form

$$U_{IIJ}(r,r')=g_{IIJ}\frac{e^{-\alpha_{IIJ}r}}{r}\frac{e^{-\alpha_{IIJ}r'}}{r'}\ ,$$

which in momentum space becomes

$$U_{IIJ}(k,k')=g'_{IIJ}v_l(\alpha_{IIJ},k)v_l(\alpha_{IIJ},k')\ ,$$

where

$$v_0(\alpha,k)=\frac{\alpha^2}{\alpha^2+k^2}$$

and

$$v_1(\alpha,k)=\frac{\alpha^2}{k^2}\tan^{-1}k/\alpha-\frac{\alpha^3/k}{\alpha^2+k^2}\ .$$

The combinations of strengths g and ranges α are determined from data and/or phase-shift analysis results for the energy range of interest here (30 MeV $<T_{\mathrm{lab}}<$ 70 MeV). The codes developed for solving the coupled channel problem of Eq. (2) are sufficiently general to handle any well-behaved nonlocal or local potential. However, the resulting eigenphases and mixing angles do not exhibit a strong dependence on the form of the potential used. This is illustrated in Fig. 1. The solid line indicates how the mixing angle ϵ_s (the s-wave channel) varies with pion energy. The potential used for the solid line was obtained by fitting the existing π-n data as described in Sec. III. The off-shell ranges obtained were $\alpha_{1/2}=225$ MeV/c and $\alpha_{3/2}=600$ MeV/c. If one were to use isospin phase equivalent potentials with different off-shell ranges, the resulting S matrix does not change significantly. The difference in the eigenphases in this energy range is less than 0.5%. We show a similar effect in Fig. 1. The dashed curve corresponds to potentials with off-shell ranges $\alpha_{1/2}=\alpha_{3/2}=300$ MeV. The potential strengths were varied as a function of energy to match the eigen-

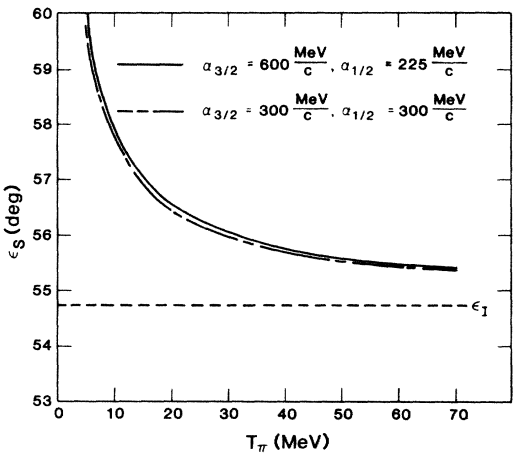

FIG. 1. Comparison of the s-wave mixing angle for two potentials with different off-shell ranges but common eigenphases.

phases of the solid curve. The resulting change in ϵ is almost negligible.

Before analyzing the two-channel system in more detail, we will consider the effect of the γn channel. This can be done for the $l=0$ partial wave, the dominant one at very low energies, by adding a third coupling and wave function, $\psi_3(\gamma n)$, to Eq. (2). ψ_3 will satisfy a similar equation to ψ_1 and ψ_2,

$$\nabla^2\psi_3+k_3^2\psi_3+\mu_3V_{13}\psi_1+\mu_3V_{23}\psi_2+\mu_3V_{33}\psi_3=0\ ,$$

where $\mu_3=E_\gamma E_n/(E_\gamma+E_n)$.

Since the γn channel is much weaker than the other two, there is very little back coupling. The amplitudes f_{13} and f_{23} are very small, and f_{13} is essentially just a Born term. Thus the above procedure is expected to be a reasonable approximation for including the third channel. In essence, the potential V_{13} determines the imaginary part of S_{13}, with adjustments to the other components of S determined by the strong 2×2 interaction and unitarity. We are using this system to determine how large these corrections are.

The three channel potential, V, will have the form

	π^-p	π^0n	γn
π^-p	V_{11}	V_{12}	V_{13}
π^0n	V_{21}	V_{22}	V_{23}
γn	V_{31}	V_{32}	V_{33}

where V_{11}, V_{12}, V_{21}, and V_{22} are determined as before. Time reversal invariance requires $V_{ij}=V_{ji}$. V_{13}, the largest of the new interactions, is taken to be the same form as the isospin potentials. The strength and range were adjusted to fit the Panofsky ratio at threshold and the experimental $\gamma n\to\pi^-p$ integrated cross section at $T_\pi=27$ MeV assuming only s waves contribute. These values are listed in Table II along with the π-N potential parameters determined in Sec. III by fitting to the data. We note that we were able to obtain the energy dependence of f_{13} by using an off-shell range of 200 MeV/c, which is of the same magnitude as that of the $S_{1/2}$ channel.

V_{23}, much smaller than V_{13} since there are no charged particles in either the initial or final state, was taken to be of the same form as V_{13} with the overall strength scaled down as determined by the multipole analysis of Berands and Donnachie.[10] That is, using the notation of Ref. 11,

$$|S_{23}|=|S_{13}|\frac{E_{0+}(\pi^0n)}{E_{0+}(\pi^-p)}\ .$$

The potential strength of V_{23} was adjusted until the above condition on the amplitudes, or S matrix elements, was satisfied. Due to the weak nature of this channel, the other amplitudes displayed little sensitivity to variations in the magnitude of V_{23}. Finally, V_{33}, which represents $\gamma n\to\gamma n$ scattering, is extremely small and was chosen to be equal to V_{11} times the ratio [fine structure constant (α)/strong coupling constant].[2] The primary aim of this exercise of including the γn channel is to estimate the effect on the eigenphases and mixing angle of the two-channel (π^-p,π^0n) system. To this end, an accurate potential is not absolutely necessary. As we shall see, the effect of the third channel on the two-channel problem is small, reducing the importance of accurate potentials. Nonetheless, the above potentials reproduce the total cross sections reasonably well. (See Table I.) These potentials can now be used to generate a 3×3 $S^{S1/2}$ matrix.

There are various ways to parametrize a 3×3 symmetric unitary matrix. Six real variables are required [3(3+1)/2], but the functional form is not unique. The choice of Waldenstrøm (Ref. 11) is to use three elastic phases and three inelastic parameters. This is useful in examining bounds on cross sections and amplitudes imposed by the constraint of unitarity. In this paper we choose a different parametric form, one that reduces, for $V_{13}=V_{23}=0$, to the form of Eq. (1). By slowly turning on the photoproduction interaction, the variables which parametrize the S matrix will vary continuously. This type of choice offers a convenient transformation between the two-channel and three-channel analysis.

Generalizing the form of Eq. (2) to three channels requires three eigenphases ($\delta_1,\delta_2,\delta_3$) and three mixing angles (ϵ,β,γ). S can be written as

$$S^{s_{1/2}}=M_3^\dagger(\epsilon,\beta,\gamma)\begin{bmatrix}e^{2i\delta_1}&0&0\\0&e^{2i\delta_2}&0\\0&0&e^{2i\delta_3}\end{bmatrix}M_3(\epsilon,\beta,\gamma)\ ,$$

where $M_3=0_{ij}e^{i\lambda_i}$ and $0\in O(3)$. However, since we are just considering the S matrix and its eigenvectors, the three phases λ_i have no physical significance. The choice in this paper is to set $\lambda_i=0$, thus $M_3\in O(3)$ with no loss of generality.

If one makes this choice of parametrization, the eigenphases are uniquely determined (up to $2\pi n$) since they are just the phases of the eigenvalues of S. There is an arbitrariness, however, as to how the mixing matrix $M_3(\epsilon,\beta,\gamma)$ is to be parametrized. Any parametrization of the group O(3) will do, so we need to consider the system at hand. In the limit of $V_{13}=V_{23}=0$, the γ-n channel is decoupled;

TABLE I. S matrix parameters (for $l=0$ partial wave).

Three-channel S matrix $(\pi^-\mathrm{p},\pi^0\mathrm{n},\gamma\mathrm{n})$

T_π (MeV)	$\delta'_{3/2}$	$\delta'_{1/2}$	δ'_0	ϵ	β	γ	$\sigma_t(\gamma\mathrm{n}\to\pi^-\mathrm{p})$ μb	f_{CEX} (fm)
10	−2.27	4.68	0.29	56.1	31.1	−3.07	102	−0.206 13−0.008 45i
30	−3.90	6.46	−0.01	54.9	26.3	−4.04	131	−0.185 16−0.007 98i
50	−5.15	7.35	−0.56	54.6	24.3	−5.22	126	−0.173 92−0.006 28i

Threshold Panofsky ratio $=1.56$

Two-channel truncated $\tilde{S}$ matrix $(\pi^-\mathrm{p},\pi^0\mathrm{n})$

T_π (MeV)	$\delta_{3/2}$	$\eta_{3/2}$	$\delta_{1/2}$	$\eta_{1/2}$	$\sin(2\epsilon)$	ϵ
10	−1.92	0.9995	4.27	0.9989	0.9016−0.0028i	57.81
30	−3.54	0.9992	6.03	0.9983	0.9267−0.0026i	56.03
50	−4.82	0.9990	6.92	0.9981	0.9325−0.0024i	55.59

Two-channel S matrix $(\pi^-\mathrm{p},\pi^0\mathrm{n})$

T_π (MeV)	$\delta_{3/2}$	$\delta_{1/2}$	ϵ	f_{CEX} (fm)
10	−1.92	4.26	57.74	−0.206 29−0.008 42i
30	−3.55	6.01	55.98	−0.185 40−0.007 98i
50	−4.83	6.91	55.55	−0.174 18−0.006 33i

$$\lim_{V_{13},V_{23}\to 0} M_3(\epsilon,\beta,\gamma)\to M_3(\epsilon,0,0)=\begin{bmatrix} & & 0\\ & M_2(\epsilon) & 0\\ 0 & 0 & 1\end{bmatrix}.$$

This suggests using the same ϵ as before to mix the (now modified) isospin $\frac{3}{2}$ and $\frac{1}{2}$ states. This angle should be the largest of the three, since the hadronic interaction (V_{11},V_{12},V_{22}) is much stronger than the electromagnetic couplings (V_{13},V_{23}). For the $(\pi^-\mathrm{p},\pi^0\mathrm{n},\gamma\mathrm{n})$ system (total charge=0), V_{13} is much larger than V_{23}, so one would expect the eigenstate of the full Hamiltonian in which the $\gamma\mathrm{n}$ state is dominant to be primarily mixed with $\pi^0\mathrm{n}$. Thus for this system the next largest mixing angle is expected to be between the $\pi^0\mathrm{n}$ and $\gamma\mathrm{n}$ physical states. Directed by these physical motivations, we will use the following form for the mixing matrix M_3:

$$M_3(\epsilon,\beta,\gamma)=\begin{bmatrix}\cos\gamma & 0 & \sin\gamma\\ 0 & 1 & 0\\ -\sin\gamma & 0 & \cos\gamma\end{bmatrix}\begin{bmatrix}\cos\epsilon & \sin\epsilon & 0\\ -\sin\epsilon & \cos\epsilon & 0\\ 0 & 0 & 1\end{bmatrix}\begin{bmatrix}1 & 0 & 0\\ 0 & \cos\beta & \sin\beta\\ 0 & -\sin\beta & \cos\beta\end{bmatrix}.$$

The last rotation (γ) is chosen to ensure $M_3(\epsilon,\beta,\gamma)$ spans the space of O(3), and for $\epsilon=0$ would be orthogonal to β. One could also choose γ along the "1" axis which would correspond to a type of Euler angle parametrization. The results of this parametrization for the $l=0$ channel are included in Table I.

These results can also be expressed pictorially as shown in Fig. 2. In this figure the three eigenstates are drawn as vectors in the space of physical states. That is, the axes are labeled $\pi^-\mathrm{p}$, $\pi^0\mathrm{n}$, and $\gamma\mathrm{n}$, which correspond to the physically observed states. Eigenstates of the full interaction (for a particular value of J^P) labeled $\nu_{3/2}$, $\nu_{1/2}$, and ν_0, are unit vectors in this space, whose projection on the axis indicates the amount of physical state in the eigenstate. The eigenvectors $\nu_{3/2}$, $\nu_{1/2}$, and ν_0 form an orthonormal basis themselves, and the mixing matrix is just the rotation matrix that transforms from the physical basis to the eigenbases

$$\begin{bmatrix}\nu_{3/2}\\ \nu_{1/2}\\ \nu_0\end{bmatrix}=M_3\begin{bmatrix}\pi^-\mathrm{p}\\ \pi^0\mathrm{n}\\ \gamma\mathrm{n}\end{bmatrix}.$$

At $T_\pi=30$ MeV, we obtain

$$M_3=\begin{bmatrix}0.574 & 0.762 & 0.299\\ -0.818 & 0.515 & 0.255\\ 0.040 & -0.391 & 0.919\end{bmatrix}$$

or

$$\psi_{3/2}=0.99\left[\frac{1}{\sqrt{3}}\right]|\pi^-\mathrm{p}\rangle+0.93(\sqrt{2/3})\,|\pi^0\mathrm{n}\rangle$$
$$+0.299\,|\gamma\mathrm{n}\rangle\,,$$

$$\psi_{1/2} = -1.00(\sqrt{2/3})\,|\pi^-\mathrm{p}\rangle + 0.89\left|\frac{1}{\sqrt{3}}\right|\,|\pi^0\mathrm{n}\rangle + 0.255\,|\gamma\mathrm{n}\rangle\,,$$

$$\psi_0 = 0.04\,|\pi^-\mathrm{p}\rangle - 0.391\,|\pi^0\mathrm{n}\rangle + 0.919\,|\gamma\mathrm{n}\rangle$$

for the $s_{1/2}$ channel. Under true isospin symmetry and no photoproduction interaction, ν_0 is along the γn axis, $\nu_{3/2}$ and $\nu_{1/2}$ lie in the π^-p-π^0n plane, and $\epsilon=\epsilon_I$. Mass differences and electromagnetic couplings cause the vectors to move in a continuous manner while remaining orthogonal, in this space. This type of diagram offers a visual representation of the π^-p,π^0n,γn system and the amount of deviation from pure isospin symmetry. One could also project these eigenvectors onto an isovector basic (i.e., ν_i under pure isospin symmetry). An equivalent diagram and analysis can be drawn for the π^+n,π^0p,γp system as well. Note that the vectors ν_i do not depend on the choice of parametrization of M_3, but only on the basic interaction of which the ν_i are eigenvectors.

Comparison with the two channel system is best done by examining the S matrix with and without the V_{13} and V_{23} coupling (for $T_{\mathrm{lab}}=30$ MeV):

$$\begin{bmatrix} (0.982\,53, 0.104\,88) & (0.0066, -0.1539) \\ (0.0066, -0.1539) & (0.987\,88, -0.0196) \end{bmatrix} \begin{bmatrix} (0.980\,01, 0.104\,89) & (0.0066, -0.1536) \\ (0.0066, -0.1536) & (0.987\,88, -0.0196) \end{bmatrix}$$

(with the former for the two-channel S and the latter for the truncated two-channel $\tilde{S}$). Even though the γ-n channel accounts for 12% of the total cross section, the 2×2 submatrix corresponding to the (π^-p,π^0n) states does not change significantly. This is due to the weakness of the interaction, and/or the low energies. Since under these conditions

$$|S_{13}|^2 = 4k^2|f_{13}|^2 \ll 1\,,$$

the reduction of S_{11} and S_{12} imposed by unitarity is very small. Most of the "loss" comes from ReS_{11}; f_{11} and $f_{12}=f_{\mathrm{CEX}}$ do not change significantly. The effect of this third channel on the charge exchange amplitude, f_{CEX}, can be seen to be only $\sim$0.15% from Table I. One can then limit the analysis to the π-nucleon system which is represented by a 2×2 slightly nonunitary S matrix for each lj channel. To quantify the degree of "two-channel" inelasticity we define a truncated S matrix, $\tilde{S}$, as follows:

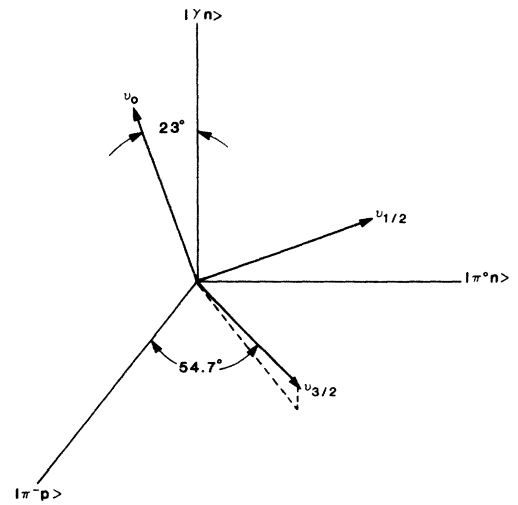

FIG. 2. Diagram of the eigenvectors of the π^-p,π^0n,γn system at $T_\pi=30$ MeV (s wave only).

	π^-p		π^0	γn
π^-n		$\tilde{S}$		S_{13}
π^0n				S_{23}
γn	S_{13}		S_{23}	S_{33}

where $\tilde{S}$ describes the (π^-p,π^0n) system.

$\tilde{S}$ is not unitary, but symmetric, and can be represented by six real parameters. The parametric form of Eq. (1) can still be used but with complex variables. That is, the six real quantities that describe $\tilde{S}$ can be chosen to be two complex eigenphases and one complex mixing angle. In Table I we present the values of these parameters for various energies, and it can be seen that the inelasticities due to photoproduction are very small ($\eta_1\sim0.9997, \eta_2=0.9990$, $\sin2\epsilon\sim0.911-0.0014i$). The errors introduced by using three real parameters are less than 0.5% for the eigenphases. The violation of unitary can also be expressed in a 2×2 matrix form:

$$\tilde{S}^\dagger\tilde{S} = \begin{bmatrix} 0.995 & (-0.000\,07, 0.000\,38) \\ (-0.000\,07, -0.000\,38) & 0.999 \end{bmatrix}$$

and is about 0.5% violation. In summary, the errors due to the exclusion of photoproduction by using a truncated S matrix, $\tilde{S}$, are very small for $30<T_\pi<70$, and the parametrization of $\tilde{S}$ ($\delta_{3/2}$,$\delta_{1/2}$,ϵ) using real parameters is accurate to within 0.5%. In the following analysis in this paper we will parametrize $\tilde{S}$ according to Eq. (1), with real parameters.

III. DATA ANALYSIS

Since only very limited charge exchange data have been available until recently, the standard procedure has been to perform a phase shift analysis on both π^+p and π^-p elastic scattering and make use of isospin invariance to predict the change exchange amplitudes. The usual problems exist for phase shift analyses, principally that data sets taken from the literature tend to be inconsistent, which means that unspecified systematic errors are

present. Because the data presented to the χ^2 analysis manifestly violate the assumed conditions for statistical treatment, the mathematical framework of such tests is rendered almost useless. Of course one continues to use the methods in spite of this, having no good way to choose between contradictory data sets.

The existence of new high-quality charge exchange data has altered this situation drastically. Assuming isospin invariance in the strong interaction, there is now a redundancy available to check the consistency of data sets. First, we must determine that the charge exchange data form a consistent set. Using the measurements of Fitzgerald *et al.*[12] (seven energies, three forward angles per energy), Salomon *et al.*[13] (integrated charge exchange at two energies), and Duclos *et al.*[14] (180° charge exchange at three energies) we have a data set consisting of 26 points. Expressing the CEX amplitude as an s- and p-wave polynomial in pion-nucleon center of mass momentum, it is easy to show that a χ^2 fit of less than 1 per degree of freedom is possible. Thus at least the data set is not internally inconsistent. We have chosen to apply the formalism presented in Sec. II to these data, as well as the elastic scattering data, but the χ^2 criterion was applied only to the CEX data.

Since the charge exchange amplitude determines only the difference between the isospin $\frac{3}{2}$ and $\frac{1}{2}$ amplitudes, we started with a representation of the current isospin $\frac{3}{2}$ amplitudes. The P_{33} phase shift was kept fixed, but the $S_{3/2}$ and the P_{31} were allowed to vary slightly to improve the fit to the charge exchange data.

The resulting phase shifts are shown in Figs. 3–5. Most of the values are in reasonable agreement with previous determinations. Note that the P_{31} does not agree very well at high energies. The charge exchange data favor this large P_{31}. However, using the dashed curve in Fig. 4 for $\delta_{P_{31}}$, and including d waves from Ref. 15, we were also able to obtain a low χ^2/N for the charge exchange data. An analysis was done for each of these conditions, one using just s and p waves with P_{31} represented by the

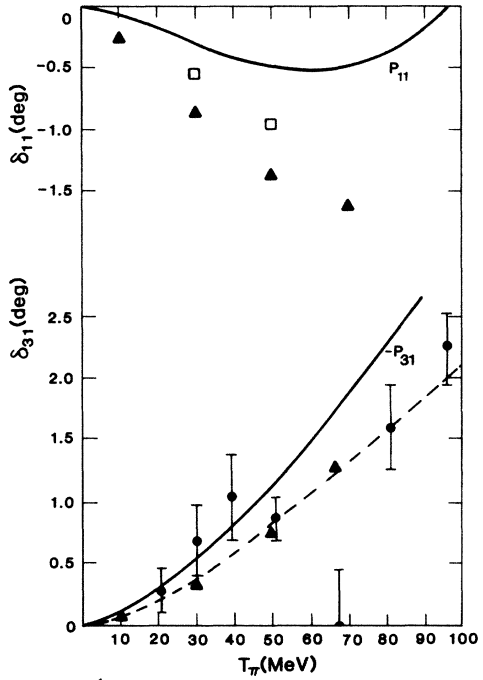

FIG. 4. Spin $\frac{1}{2}$ p-wave pion-nucleon phase shifts. The circles are from Ref. 15, the triangles from Ref. 16, the boxes from Ref. 17.

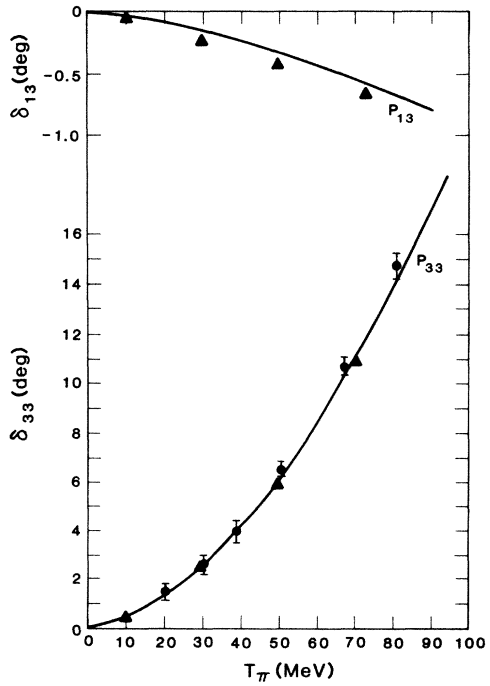

FIG. 3. Spin $\frac{3}{2}$ p-wave pion-nucleon phase shifts. The circles are from Ref. 15, the triangles from Ref. 16.

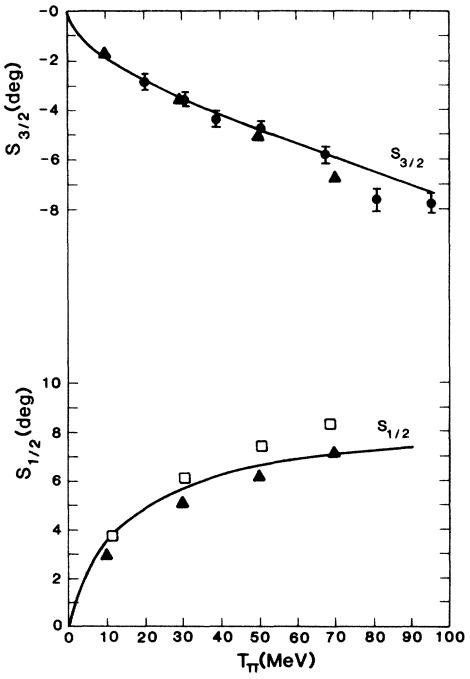

FIG. 5. s-wave pion-nucleon phase shifts. The circles are from Ref. 15, the triangles from Ref. 16, the boxes from Ref. 17.

solid line in Fig. 4 and another using the dashed line for P_{31} plus the d waves from the analysis of Ref. 16.

Comparisons with π^+p elastic scattering are given in Figs. 6–9. It is seen that, in most cases, agreement and consistency are good. Notable exceptions are the forward angles at high energy and the comparison with the Frank *et al.*[19] data at 29.4 MeV. Part of the discrepancy at the high energy is caused by the large P_{31} phase. Reducing this phase shift and including the d waves increases the back angles, and decreases the forward angle cross sections by 5% and 7%, respectively, at 67 MeV.

Using these isospin $\frac{3}{2}$ phase shifts, the isospin $\frac{1}{2}$ values of the range and strength were varied to give a best fit to the CEX data. A basic ambiguity comes about from the range of the $S_{1/2}$ potential. It has long been recognized that this phase shift deviates strongly from a pure scattering length approximation even at low energies. This is an indication that the interaction range is large. One would like to determine the charge exchange scattering length (i.e., the combination of the two isospin scattering lengths which would represent charge exchange scattering if isospin were strictly conserved) from this data. In principle one can compare the s-wave amplitude to the p-wave amplitude very accurately at the forward angle cancellation point, and in fact this comparison is independent of data normalization errors, to first order, since only the energy of the minimum need be known accurately. To see how this works ideally, consider the real part of the non-spin-flip charge exchange amplitude to be parametrized in the scattering-length–scattering-volume form valid at low energy

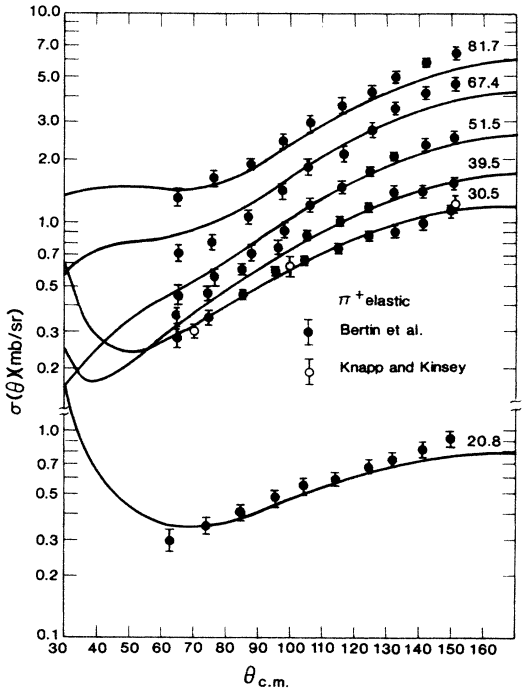

FIG. 6. Comparison of π^+p cross sections from the present calculation with the data of Bertin *et al.* (Ref. 15) and Knapp and Kinsey (Ref. 18).

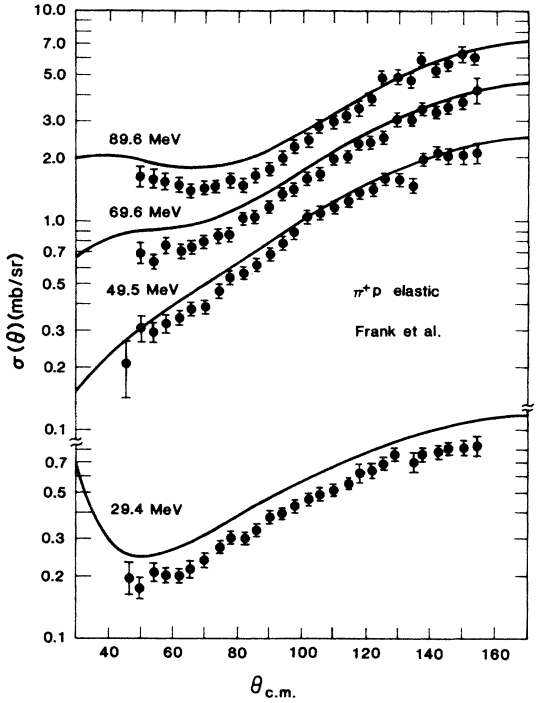

FIG. 7. Comparison with the data of Frank *et al.* (Ref. 19).

$$f(\theta)=a+ck^2\cos\theta\ .$$

Since a and c have opposite signs, it is only necessary to know (1) the value of c and (2) the energy at which $f(0)=0$, to determine a, the desired quantity. The value of c is dominated by the P_{33} phase shift and is reasonably well known from higher energy data. At some level the limits of accuracy will be determined by the uncertainties in c.

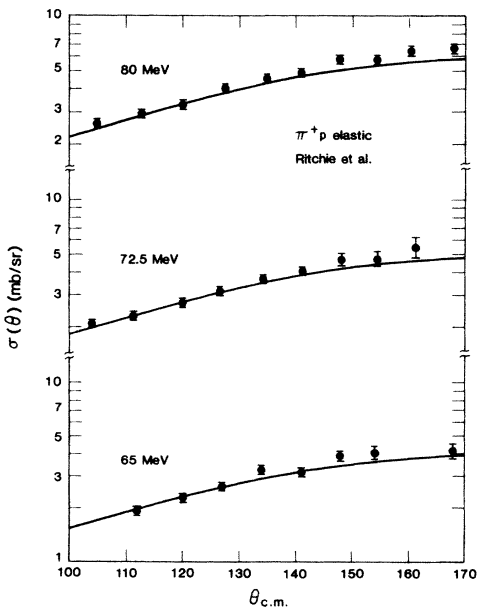

FIG. 8. Comparison with the data of Ritchie *et al.* (Ref. 20).

This simple picture is destroyed, however, by the fact that the $S_{1/2}$ amplitude has a large effective range, forcing us to modify the simple form and to write

$$f(0)=a+bk^2+ck^2\cos\theta\ .$$

At zero degrees a will be compared with the sum of b and c. Thus, there is an ambiguity corresponding to different values of a and b but with the same sum for $a+bk^2_{\min}$. This effect is clearly seen in the χ^2 contour plot of Fig. 10, where at the minimum point, $\chi^2/N=22/26$, from the data sets of Refs. 12–14. The horizontal axis represents the range parameter for the $S_{1/2}$ potential, and the vertical axis could well have been the strength of this potential, but we have chosen instead to label it by the value of the CEX scattering length that would be obtained with equal masses and no Coulomb field so that a direct comparison can be made. It is clear that, if this effective range ambiguity did not exist, the scattering length could be determined very accurately ($\sim\pm0.001$ fm). As things stand, with the charge exchange data alone the best that can be done is

$$a=-0.193\pm0.005\text{ fm}\ .$$

Converting to the usual normalization and units (inverse pion masses), the odd scattering length (a_1-a_3) is $a^-=0.290\pm0.008\ \mu^{-1}$. We defer a more detailed discussion of this value to later in the section.

Since we have determined all of the pion-nucleon phase shifts and we have a way of correcting for Coulomb effects, we are now in a position to *predict* the π^--p scattering cross section. This is of particular interest since the latest, and presumably highest quality, data recently published by Frank *et al.*[19] disagree rather strongly with phase shift predictions based on previous data. One is faced with the apparent dilemma of having to deny *all* of

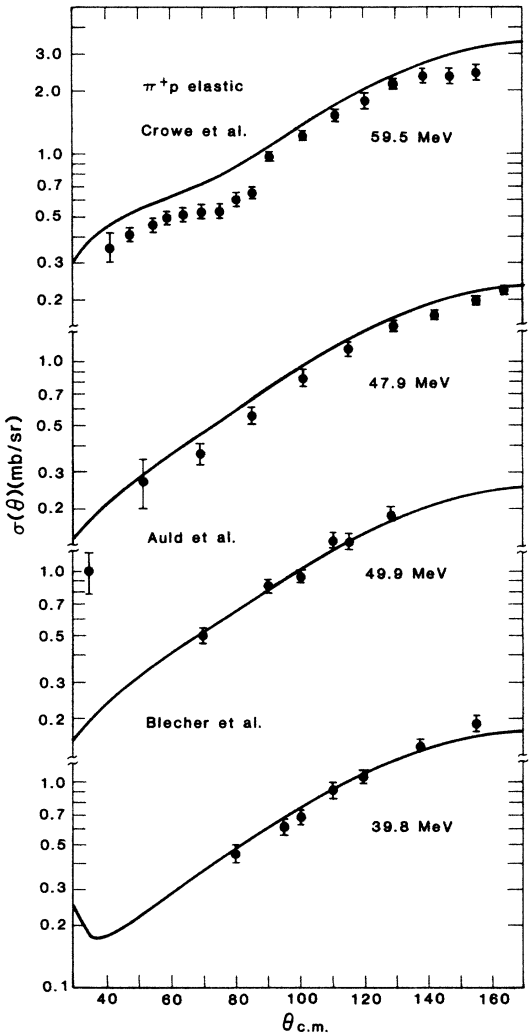

FIG. 9. Comparison with the data of Blecher *et al.* (Ref. 21), Auld *et al.* (Ref. 22), and Crowe *et al.* (Ref. 23).

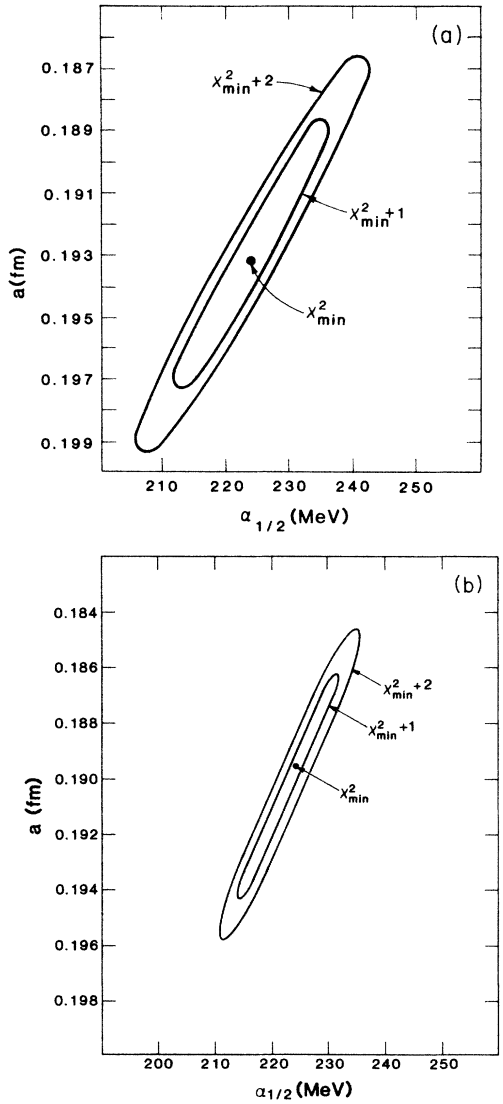

FIG. 10. (a) Contour map of the χ^2 surface from comparison with charge exchange data showing the ambiguity between "a" and the $S_{1/2}$ off-shell range. The minimum value of χ^2 is 23.7 for 26 data points. (b) Similar contour map fitting the three highest energies of the Frank data. The minimum value of χ^2 is 197 for 82 data points.

the existing previous data in order to accept the data of Ref. 19 or else discard what should be the best data available. As we shall see, this apparent problem is mostly an illusion.

The first step is to compare our predictions based on (1) average $\frac{3}{2}$ phase shifts, (2) isospin invariance (with our correction for known isospin breaking effects assumed to be adequate), and (3) the recent charge exchange data, with the Frank *et al.*[19] π^--p data. This comparison is shown in Fig. 11. As may be seen, the agreement is remarkably good, especially for the three highest energies. In fact, for these three energies the representation is good even in a χ^2 sense, probably somewhat better even than the π^+p data on which it is based. The χ^2/N for the 49.6, 69.6, and 89.6 MeV data sets are 103/28, 66/27, and 51/27, respectively (statistical errors only). Does this mean that the rest of the existing data on low energy π^-p scattering are wrong? To answer this question we show the comparisons of our predictions with the other existing sets of π^-p data. Figure 12 shows comparisons with three sets of data. These data are in as good an agreement with our predictions as they could be with any smooth curve or with each other.

If we compare with the data of Crowe *et al.*,[23] however, the situation is very different. (See Fig. 13.) The small error bars quoted cause a strong disagreement with the prediction. Since this is all of the differential cross section data usually used below 98 MeV, it seems that one data set was determining, almost entirely, the isospin $\frac{1}{2}$ phase shifts. Perhaps it is worth noting that these data were taken incidentally to the main experiment, which was to measure $\pi^{\pm}$ ^{4}He elastic scattering, and that the entire published description of the hydrogen data experiment is contained in a single paragraph. It might also be

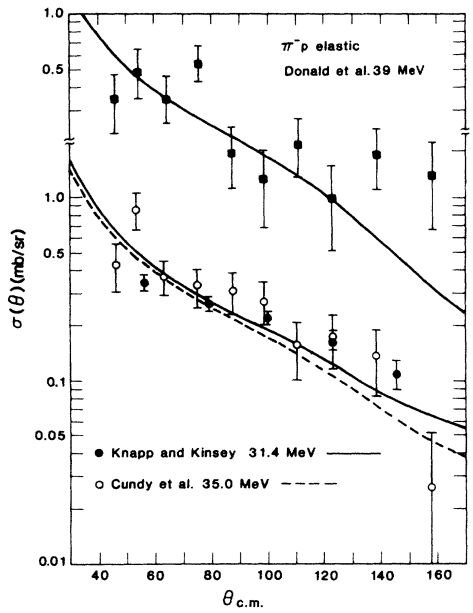

FIG. 12. Comparison of our predictions for π^-p scattering with three early data sets: Knapp and Kinsey (Ref. 18), Cundy *et al.* (Ref. 24), and Donald *et al.* (Ref. 25).

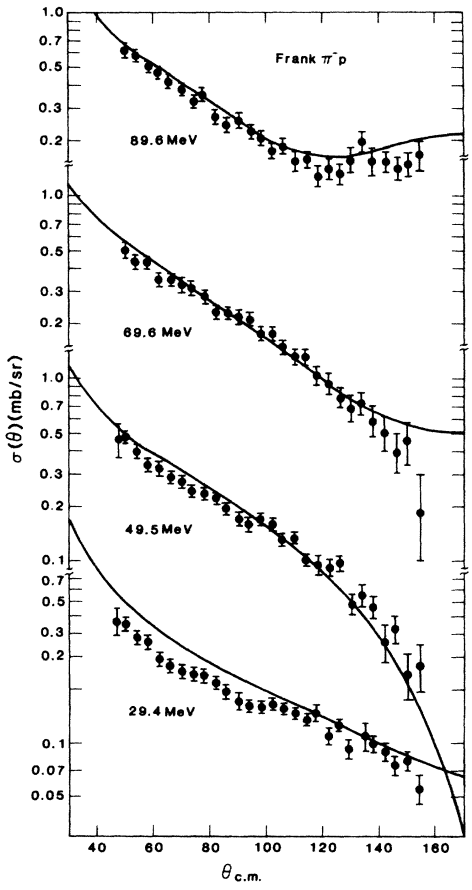

FIG. 11. Comparison of the prediction of the present calculation for π^-p scattering with the data of Frank *et al.* (Ref. 19).

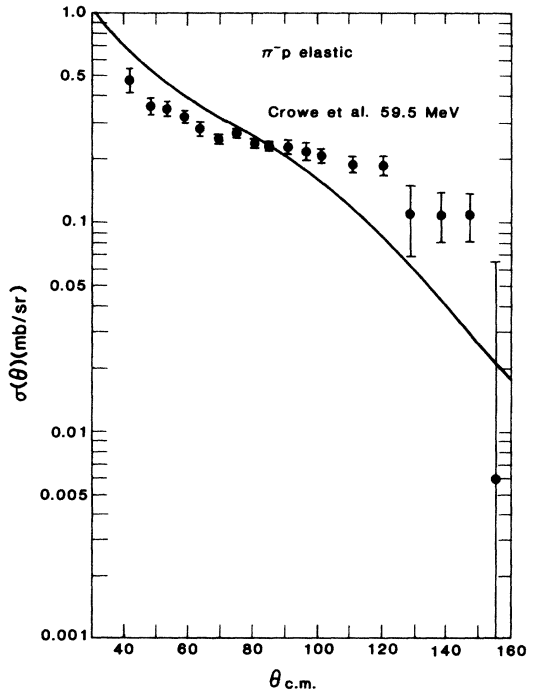

FIG. 13. Comparison of our predictions for π^-p scattering with the data of Crowe *et al.* (Ref. 23).

noted that, when published, it disagreed with all previous phase shift analyses. Extending our calculations up to 98 MeV and comparing to the data of Edwards *et al.*,[26] we obtain fair agreement at the forward angles but are low by about 20% at the larger angles. This energy is beyond the limits of the model, especially for the P_{11} phase shift. Even so, due to the small difference in energy between these data and those of Ref. 19 there would appear to be a discrepancy.

Given the conditions mentioned above we see no reason not to have confidence in the three highest energies of both π^+p and π^-p data taken by Frank *et al.*[19]

The data at 30 MeV are much harder to understand. Note that both sets of data ($\pi^\pm$) are consistent with the *same* renormalization of 20—30%, i.e., *both* data sets lie below the present predictions. We now argue that it is very difficult (impossible?) to imagine changing the strong interaction phase shifts in any way so as to fit both data sets.

This statement is based on the observation that the charge exchange measurement fixes the difference between the isospin $\frac{3}{2}$ (f_3) and isospin $\frac{1}{2}$ (f_1) amplitudes. Thus if one changes f_3, e.g.,

$$f_3 \rightarrow f_3 + \delta \, ,$$

then, in order to keep the same charge exchange amplitude ($\sim f_3 - f_1$) invariant, one must change f_1 accordingly,

$$f_1 \rightarrow f_1 + \delta \, .$$

It follows that the π^- amplitude changes by the same amount. Consider, for example, the 29.4 MeV π^-p data at 50°. Here the spin flip portion of the cross section is negligible (0.013 mb/sr compared to 0.580 mb/sr). The Coulomb amplitude is 0.099 fm and the real part of the strong amplitude is 0.158 fm. In order to reduce the cross section to the observed value of 0.45 mb/sr, the strong amplitude would have to be decreased to 0.113 fm, a change of -0.045 fm. Applying this same change to the π^+p amplitude, which is -0.027 fm, and including the Coulomb amplitude (-0.099 fm), one arrives at a non-spin-flip cross section of 0.292 mb/sr, which is much larger than the data (~ 0.2 mb/sr) even without the 0.087 mb/sr spin-flip cross section. The basic reason for this behavior is the interference of the Coulomb amplitude. Since it enters with the opposite sign in the two cases, improving the agreement with one cross section will always make the other worse.

We should emphasize that the previously mentioned value for the odd scattering length (0.290 ± 0.008 μ^{-1}) was determined from a χ^2 search on the data set of Refs. 12—14 only. We have also done a similar search on the three highest energies of the Frank data. Although this elastic π^-p scattering is not expected to have a strong dependence on the odd scattering length, having fixed the $I = \frac{3}{2}$ phases, a large sensitivity can be seen in Fig. 10(b). Here, $\chi^2_{\min}$ occurs for values of $\alpha = 225$ MeV and $a = -0.1895$ fm or $a^- = 0.284$ μ^{-1}, with a value of $\chi^2/N = 2.4$. This provides an additional numerical statement of the consistency of the high energy Frank data with the charge exchange data.

Our value for the odd scattering length, 0.290 ± 0.008 μ^{-1}, can be compared with other analyses. In their compilation of pion nucleon parameters Pilkuhn *et al.*[27] list results from various groups but recommend $0.290 + 0.01/-0.02$ μ^{-1}. However, there are a number of lower values clustering around 0.26—0.27 μ^{-1} (see Ref. 13). Some of these use pion-nucleon data which do not include the latest scattering measurements. We note that previously the analysis of π^+ and π^- scattering data gave values near 0.26 μ^{-1}, but the data of Frank *et al.*[19] give substantially the same value (0.284 ± 0.005 μ^{-1}) as the charge exchange.

The analysis of the recent charge exchange experiment by Salomon *et al.*[13] obtains two values around 0.26 μ^{-1}. However, these values are extracted from the phase shifts at finite energy, i.e., assuming that the scattering length limit has been reached and that the charge exchange cross section is a constant from 27 MeV down to zero energy. Using our energy dependence for the *s*-wave phase shifts, their values and ours are consistent. In fact their integrated CEX cross section was included in our analysis.

A persistent discrepancy has existed for many years between the odd scattering length obtained from pion charge exchange and that obtained with the use of the Panofsky ratio[28] (P). In order to make this comparison one must know the value of P and the zero energy limit of the cross section for $\pi^- + \mathrm{p} \rightarrow \mathrm{n} + \gamma$ (with Coulomb effects removed). In practice this limit is obtained from detailed balance and measurements of R (the ratio of $\gamma + \mathrm{n} \rightarrow \pi^- + \mathrm{p}$ to $\gamma + \mathrm{p} \rightarrow \pi^+ \mathrm{n}$) from deuteron targets and the extrapolation of the photoproduction cross section on the proton. While there may be some problem with extrapolating R to zero energy (Coulomb and deuteron effects must be removed), we will assume (along with Ref. 28) that the number $R = 1.34 \pm 0.02$ is correct. The value of P is accurately known to be 1.546 ± 0.009.[28]

The relevant photoproduction cross section is considerably less well known. The needed quantity is actually the cross section with the phase space ratio removed:

$$\sigma'(q_\pi) = \frac{k_\gamma}{q_\pi} \sigma(\gamma \mathrm{p} \rightarrow \pi^+ \mathrm{n}) \, .$$

In Fig. 14 the quantity σ' is plotted as a function of pion momentum. The data are those of Adamovich *et al.*[29] The dotted curve is their fit based on a polynomial in pion momentum which represents these points and higher energy data as well (which is mainly p wave). This is essentially the same extrapolation as that used to get the zero energy value of the cross section (193 μb) or equivalently $E_{0+}(\pi^+)(0.283$ $\mu^{-1})$ used in Ref. 28 to get $a_1 - a_3 = 0.263 \pm 0.005$ μ^{-1}.

The solid curve shows our calculation for the cross section using a range of 200 MeV/c for the V_{13} coupling potential and a strength adjusted to give a correct Panofsky ratio. For these low energy data points we obtain a better χ^2/N than Ref. 29. Note that we fit the recently measured point of Salomon *et al.*[13] at 27.4 MeV. Since our calculations are *s* wave only and we have not performed a multipole analysis, our results may be too high at $q = 0.4$

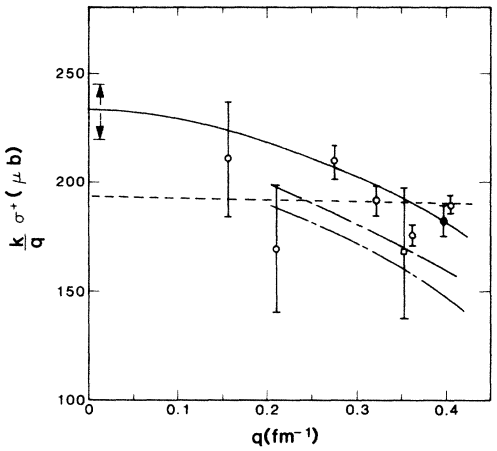

FIG. 14. Comparison of our calculation with measured photoproduction cross section and the analysis of Berends *et al.* The arrows correspond to the uncertainty quoted for our extracted value of the odd scattering length. The open circles are from Ref. 29, the solid circle from Ref. 13, and the square from Ref. 30.

fm^{-1}. Two different analyses by Berends *et al.*[10,31] (based only on data) give a very similar energy dependence but a slightly smaller magnitude. This energy dependence is perhaps the most interesting aspect of the work. We find that it comes about naturally from the inclusion of the finite size for the pion-nucleon system of the order of 1 fm. It is not clear if this should be interpreted as a bag size or if it is due to the pion cloud, but in any case it is a fundamental length scale of the pion-nucleon system. We note that a π-nucleon scattering mechanism in which the pion scatters off of the pion cloud of the nucleon can proceed only through the $I=\frac{1}{2}$ channel. This is because the π-π interaction at low energies is primarily $I=0$ (the $I=2$ scattering length is an order of magnitude smaller). The photoproduction reaction can also proceed via the pion cloud. Therefore, in this simple picture, the $S_{1/2}$ and γ-n potentials would have roughly the same range (about 1 fm, or $\alpha \sim 200$ MeV) and both be longer than the $I=\frac{3}{2}$ channel, which might correspond to a "bag-size" length scale.

Another recent value of σ' $[E_{0+}(\pi^+)]$ at zero energy is that of Noelle and Pfeil:[32] 223 μb (0.298 μ^{-1}). This is to be compared with our values of 232 ± 13 μb (0.304 ± 0.008 μ^{-1}). Thus we are in agreement with photoproduction cross sections from Ref. 32.

Our conclusion with respect to the Panofsky ratio is there is no discrepancy within the quoted errors (even not including errors in R) if recent photoproduction analyses are used.

At $T_\pi=45$ MeV, where the minimum of $\sigma(0)$ occurs, the d-wave contributions (taken from Ref. 16) are about 2% of the s-wave amplitude calculated here. Including in these amplitudes and redoing the χ^2 search on the charge exchange data, we find that the minimum occurs roughly at the same position in the $a-\alpha_{1/2}$ plane of Fig. 10. We were able to obtain $\chi^2_{\min}/N \approx 1.0$ by lowering δ_{31} to the dashed curve in Fig. 4, which slightly improves the high energy π^+-p results.

We conclude this section with a remark about the potentials used. Table II lists the parameter set. Each potential has a one term separable form except for $V_{P_{11}}$, which is the sum of two terms. Two terms were necessary to obtain the energy dependence needed to fit the charge exchange data. The values of the off-shell ranges need some qualification. These ranges are determined with respect to the potential model used here, which is energy independent. The low energy data used in this analysis from two particle scattering, pion and nucleon, are not particularly sensitive to off-shell properties, as demonstrated in Fig. 1. The data do determine the energy dependence of the phases, so a phase equivalent potential with an energy dependent strength and different range could be tailored to fit the data equally well. These ranges, therefore, are a rough measure of the deviations from the scattering length limit. The long $S_{1/2}$ range derives from the energy dependence necessary to match the data, and is perhaps accounting for complicated contributions to this amplitude (crossing symmetry, etc.) Note that to obtain the same phase shift dependence with a local Yukawa potential, we found that an off-shell range for the $S_{1/2}$ potential of $\alpha=200$ MeV was necessary.

The P_{11} phase shift determined in this analysis ($0<T_\pi<80$ MeV) is significantly less than the Arndt or Karlsruhe values. We reemphasize that this analysis is valid only up to 80 MeV, and the crossing at 95 MeV cannot be considered accurate. The recent charge exchange data favor this small P_{11} phase, and the Frank data are not inconsistent with this result. We found a very strong P_{11} dependence in the χ^2 analysis of the charge exchange data.

It is encouraging that in this energy region, only two potential parameters per channel (except the P_{11}) are needed to reproduce such a wide variety of data. Perhaps

TABLE II. Potential parameters, scattering lengths, and volumes for final fit.

	$S_{1/2}$	$S_{3/2}$	P_{33}	P_{31}	P_{13}	P_{11}		V_{13}
$\frac{g}{\alpha^4}$ (fm^2)	−0.19	0.14	−1.8	0.66	0.18	0.32	−0.93	0.08
α (MeV/c)	225	600	325	300	300	200	800	200
	a_1	a_3	a_{33}	a_{31}	a_{13}	a_{11}		$E_{0+}(\pi^-)$
	$+0.191$ μ^{-1}	-0.098 μ^{-1}	0.194 μ^{-3}	-0.033 μ^{-3}	-0.014 μ^{-3}	-0.054 μ^{-3}		-0.0350 μ^{-1}

parametrizing the potentials is more efficient than parametrizing the amplitudes or the K matrix in the energy range considered here. The separable form chosen in this paper was motivated by its applications to nuclear physics, but a potential based more on underlying physics could be employed.

IV. PION SINGLE CHARGE EXCHANGE

Using the formalism presented in Sec. II and the data analysis of Sec. III we are now prepared to calculate the charge exchange cross sections needed for pion single- and double-charge exchange on nuclei, i.e., besides the measured $\pi^-p\to\pi^0n$ we need $\pi^+n\to\pi^0p$, $\pi^0n\to\pi^-p$, and $\pi^0p\to\pi^+n$. The last two are needed for the calculation of pion analog and nonanalog double charge exchange and can be obtained from detailed balance. To calculate $\pi^+n\to\pi^0p$ it is only necessary to change the masses and Coulomb potential in the coupled channel system. One does not expect much difference in these cross sections at resonance energies, but at low energies, especially if a sharp structure occurs (like the sharp minimum around 46 MeV), then these known isospin breaking effects will play an important role.

Figure 15 shows what happens to the position of the minimum for these various reactions. We note that the $\pi^+n\to\pi^0p$ minimum occurs lower in pion laboratory kinetic energy than that for the $\pi^-p\to\pi^0n$ by about 1.5 MeV. This is interesting in view of the fact that the minimum in the lightest nuclear system measured (^{7}Li) is shifted to lower energies also, and the present calculation presumably explains some of that effect. The sensitivity to mass differences is also displayed.

Corresponding effects in the angular distribution at 50 MeV are seen as well in Fig. 16. Note that certain nuclear cases strongly select the non-spin flip (NSF) [e.g., $^{14}C(\pi^+,\pi^0)^{14}N_{2.31}$ is completely NSF, $^{13}C(\pi^+,\pi^0)^{13}N_{g.s.}$ has only $\frac{1}{9}$ SF], while others are all spin flip [e.g., $^{14}C(\pi^+,\pi^0)^{14}N_{3.95}$]. Conclusions drawn from the shape of the forward angle angular distribution depend crucially on starting from the correct free process.

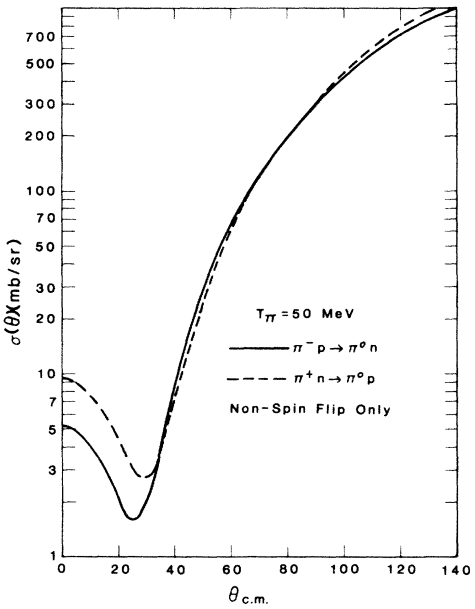

FIG. 16. Comparison of the angular distribution at 50 MeV for $\pi^-p\to\pi^0n$ and $\pi^+n\to\pi^0p$. Only the non-spin-flip cross section is shown.

Even the integrated cross section will show strong effects if the energy is low enough. Figure 17 shows the results extended down to 100 keV where order of magnitude changes occur. At energies above 800 keV the process with the larger final phase space gives the larger cross section, but below that energy the Coulomb effect becomes dominant. Note that even at 10–20 MeV deviations from the isospin predictions are significant.

We present a polynomial representation of these amplitudes which gives a reasonable representation of the data around the minimum ($\sim$30–60 MeV). These amplitudes

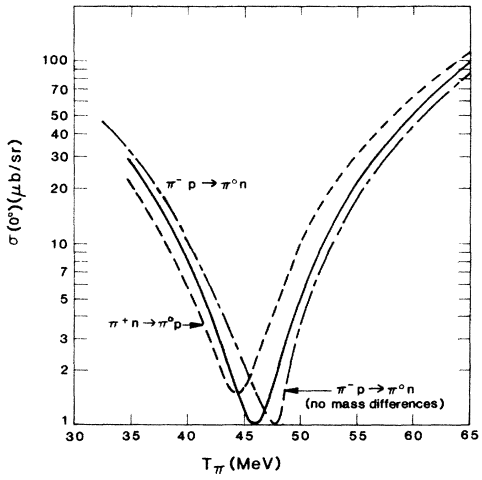

FIG. 15. Comparison of the 0° differential cross section for $\pi^+n\to\pi^0p$ and $\pi^-p\to\pi^0n$.

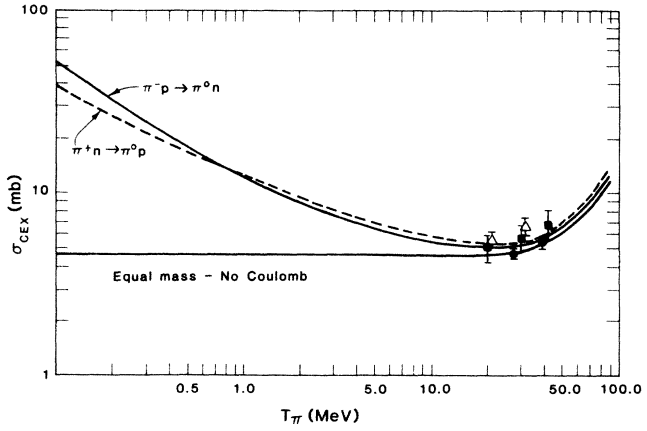

FIG. 17. Comparison of the integrated cross sections for $\pi^-p\to\pi^0n$ and $\pi^+n\to\pi^0p$. The data points are as follows: open circles, Ref. 13; open squares, Ref. 33; open triangles, Ref. 34. Only the data from Ref. 13 were included in the fit.

have the form

$$f_{NF}(\theta)=f_0+f_1\cos\theta\ ,$$

$$f_{SF}(\theta)=\tilde{f}_1\sin\theta\ ,$$

$$\sigma(\theta)=10[\,|f_{NF}(\theta)|^2+|f_{SF}(\theta)|^2]\ .$$

The f's are given in fm and the factor of 10 converts to mb/sr.

The values of f are as follows:

$\pi^-p\to\pi^0n$:

$$f_0=-0.1983+0.0810k^2-0.0068i\ ,$$

$$f_1=0.6554k^2-0.034k^4+0.4325ik^5\ ,$$

$$\tilde{f}_1=0.3826k^2+0.2025ik^5\ ;$$

$\pi^+n\to\pi^0p$:

$$f_0=-0.2000+0.0848k^2-0.0054i\ ,$$

$$f_1=0.7037k^2-0.119k^4+0.5016ik^5\ ,$$

$$\tilde{f}_1=0.3905k^2+0.2411ik^5\ ;$$

where k is the charged pion momentum in the center of mass in units of fm^{-1}. The amplitudes can also be written in a separable form:

$$f=\lambda_0(\sqrt{s}\,)+\lambda_1(\sqrt{s}\,)\mathbf{k}\cdot\mathbf{k}'\ ,$$

where k' is the π^0 momentum in the center of mass and $\sqrt{s}$ is the total invariant energy for use as a charge exchange operator. In this form, the λ's are nearly the same for the two systems.

V. CONCLUSIONS

Within the coupled channel potential model framework we can conclude the following:

1. The available single charge exchange data for $T_\pi<80$ MeV is self-consistent, and furthermore is consistent, using isospin invariance, with most π^+p and π^-p elastic scattering data in that energy region.

2. The γn channel can be ignored when parametrizing π^-p elastic and charge exchange for 20 MeV $<T_\pi<$ 70 MeV to the level of 1%.

3. Isospin breaking effects due to the Coulomb interaction and mass differences must be included in any data analysis containing pion charge exchange near 45 MeV.

4. The values of a_1–a_3 from low energy charge exchange and elastic scattering data are consistent and in agreement with recommended values from dispersion relations. They are also in agreement with the determination from the Panofsky ratio if the appropriate extrapolation to zero energy of the photoproduction data is used.

ACKNOWLEDGMENTS

We would like to thank D. Fitzgerald for the use of his data before publication. We also thank B. Ritchie, L. Heller, M. Singham, and W. B. Kaufmann for helpful conversations. This work was supported by the U.S. Department of Energy, Associated Western Universities, and Achievement Awards for College Scientists.

[1]F. Irom *et al.*, Phys. Rev. Lett. **55**, 1862 (1985).
[2]L. Van Hove, Phys. Rev. **88**, 1358 (1952).
[3]G. C. Oades and G. Rasche, Helv. Phys. Acta **44**, 5 (1971).
[4]H. Zimmerman, Helv. Phys. Acta **48**, 191 (1975).
[5]G. Rasche and W. S. Woolcock, Helv. Phys. Acta **45**, 642 (1972).
[6]G. Rasche and W. S. Woolcock, Helv. Phys. Acta **49**, 435 (1976).
[7]G. Rasche and W. S. Woolcock, Helv. Phys. Acta **49**, 455 (1976).
[8]G. Rasche and W. S. Woolcock, Helv. Phys. Acta **49**, 557 (1976).
[9]J. M. Blatt and L. C. Biedenharn, Phys. Rev. **86**, 399 (1952).
[10]F. A. Berends and A. Donnachie, Nucl. Phys. **B84**, 342 (1975).
[11]S. Waldenstrøm, Nucl. Phys. **B77**, 479 (1974).
[12]D. H. Fitzgerald *et al.* (unpublished).
[13]M. Salomon, D. F. Measday, J.-M. Poutissou, and B. C. Robertson, Nucl. Phys. **A414**, 493 (1984).
[14]J. Duclos *et al.*, Phys. Lett. **B43**, 245 (1973).
[15]P. Y. Bertin *et al.*, Nucl. Phys. **B106**, 341 (1976).
[16]R. A. Arndt, SAID on-line program.
[17]*Handbook of Pion-Nucleon Scattering* (Fachinformationszentrum, Karlsruhe, 1979).
[18]D. E. Knapp and K. F. Kinsey, Phys. Rev. **131**, 1822 (1963).
[19]J. S. Frank *et al.*, Phys. Rev. D **28**, 1569 (1983).
[20]B. G. Ritchie *et al.*, Phys. Lett. **B125**, 128 (1983).
[21]M. Blecher *et al.*, Phys. Rev. C **20**, 1884 (1979).
[22]E. G. Auld *et al.*, Can. J. Phys. **57**, 73 (1979).
[23]K. M. Crowe *et al.*, Phys. Rev. **180**, 1349 (1969).
[24]C. C. Cundy *et al.*, Proc. Phys. Soc. London **85**, 257 (1965).
[25]R. A. Donald *et al.*, Proc. Phys. Soc. London **87**, 445 (1966).
[26]D. N. Edwards, S. G. F. Frank, and J. R. Holt, Proc. Phys. Soc. London **73**, 856 (1959).
[27]H. Pilkuhn *et al.*, Nucl Phys. **B65**, 460 (1973); for a more recent compilation see Nucl. Phys. **B216**, 277 (1983).
[28]J. Spuller *et al.*, Phys. Lett. **67B**, 479 (1977).
[29]M. I. Adamovich *et al.*, Yad. Fiz. **9**, 848 (1969) [Sov. J. Nucl. Phys. **9**, 496 (1969)].
[30]D. White *et al.*, Phys. Rev. **120**, 614 (1960).
[31]F. A. Berends *et al.*, Nucl. Phys. **B4**, 1 (1967); F. A. Berends and D. L. Weaver, *ibid.* **B30**, 575 (1971).
[32]P. Noelle and W. Pfeil, Nucl. Phys. **B31**, 1 (1971).
[33]W. J. Spry, Phys. Rev. **95**, 1295 (1954).
[34]K. Miyake, K. F. Kinsey, and D. E. Knapp, Phys. Rev. **126**, 2188 (1962).